Proceedings World Geothermal Congress 2010
Bali, Indonesia, 25-29 April 2010

History Matching Simulation of the Ogiri Geothermal Field, Japan

Ryuichi Itoi[a], Yurie Kumamoto[a], Toshiaki Tanaka[a] and Junichi Takayama[b]

[a]Department of Earth Resources Engineering, Kyushu University, 744 Motooka, Nishiku, Fukuoka, 819-0395, Japan

[b]Nittetsu Kagoshima Geothermal Co., 4-2-3 Shiba, Minatoku, Tokyo, 108-0014, Japan

itoi@mine.kyushu-u.ac.jp

Keywords: Reservoir simulation, history matching, numerical model, Ogiri geothermal field, Japan.

ABSTRACT

History matching simulations were carried out for the Ogiri geothermal field with two kinds of numerical model: porous medium model and MINC model. The MINC method was applied to the grid blocks of shallow zone where steam-water two-phase condition remains during exploitation stage. Other grid blocks were treated the same as in the porous medium model. Simulated results with the MINC model show better match with pressure and temperature data at one monitoring well located in the shallow zone of reservoir.

1. INTRODUCTION

The Ogiri geothermal field has been producing steam and water since 1996. Nittetsu Kagoshima Geothermal Co. (NKGC) has developed the field and supplies steam to a power plant with installed capacity of 30 MWe operated by Kyushu Electric Power Co. At present, the number of production and reinjection wells are 15 and 9, respectively, while they were 10 and 7 when the operation of the plant was started (JGEA, 2000). The steam production rate is 275 t/h and the separated hot water at 130°C for reinjection is 875 t/h. The power plant has maintained a high average utilization efficiency of 96.2% for about 9 years since the commencement of the plant operation in March 1996. (Horikoshi et al., 2005). Thus, the Ogiri geothermal field has been operating more than ten years.

In order to design a proper and sustainable exploitation program for the field, reservoir engineering studies have been conducted since the beginning of the development. For an example, Hazama et al. (1988) developed a three-dimensional numerical model of porous medium type that was used for reservoir capacity assessment for steam production for 30 years. A simulation study for investigating evolution of a two-phase zone in a reservoir was conducted by Yano and Ishido (1995). They used a two-dimensional model of porous medium type for a sensitivity study to examine the effects of deep mass recharge and permeability of the fractured zone above the main reservoir. These studies were carried out in the exploration stage when the field had not yet started in full production (which it did in 1996), thus reservoir performances and its history under full production operation was not evaluated. Horikoshi et al. (2005) analyzed a geothermal structure of Ogiri using the data of geophysical surveys such as magnetotellulic (MT), self potential and micro-earthquake which were conducted after the start of plant operation, and concluded that high temperature geothermal fluids are recharged into the Ginyu fault reservoir, the main reservoir of Ogiri, from the east of Ogiri and most of the reinejcted water flows out the system westward. They also analyzed reservoir pressure change with time and estimated the total amount of high temperature fluid recharge to be about 1100t/h. Kumamoto et al. (2008a, 2008b, 2009) carried out a series of reservoir simulation studies that were focused on developing a numerical reservoir model to explain reservoir performance during production and reinjection in the field.

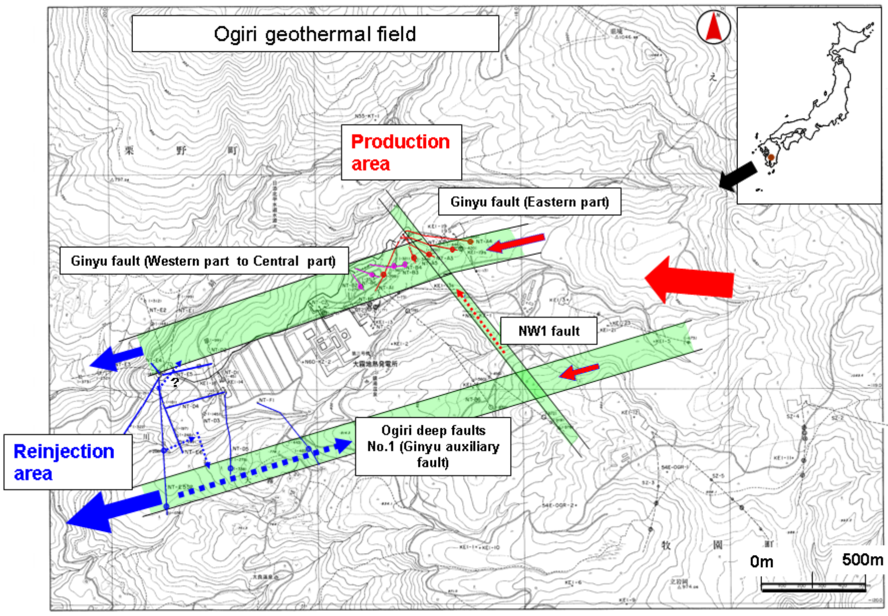

Figure 1: Plan view of Ogiri geothermal field. Red and blue arrows indicate estimated flow direction of high temperature fluid and reinjected water, respectively.

In this study, we conducted the history matching simulation of Ogiri using two kinds of numerical model, and compared their results with pressure and temperature measurements in the two observation wells.

2. RESERVOIR CHARACTERISTICS

Goko (2000) conducted geological and geochemical studies on geothermal systems of the Ogiri geothermal field in West Kirishima, Kyushu, Japan. The Ogiri area is characterized by the presence of ENE-WSW trending faults such as Ginyu and Sakkogawa faults. Figure 1 shows a plan view of the Ogiri geothermal field with wells and fault zones, and estimated flow directions of reinjected water and high temperature fluid. The Ginyu fault zone has been one of the main reservoirs targeted for development in Ogiri (Goko, 2000; Horikoshi et al., 2005). Vertical temperature profiles of wells at static conditions indicate that the reservoir has a relatively uniform temperature distribution of 230 to 232^{o}C at depths below 0 m a.s.l. (meters above sea level) and is overlain by low permeable zone that has thickness from 200m to 400m, and temperature 50 to 130 ^{o}C. Fractures in this low permeable zone are filled with hydrothermal alteration minerals. This low permeable zone acts as a cap rock in Ogiri area and prevents low temperature groundwater or meteoric water flowing downward into the reservoir. Geothermal fluid of the reservoir is of near neutral pH and chloride type. Geothermal fluids are produced from wells drilled along the Ginyu fault zone and their feed point depths range from -77m to -483m a.s.l. (Goko, 1995). The Ogiri geothermal reservoir also has the following characteristics; 1) a high permeable zone extends along the Ginyu fault, 2) a steam water two-phase zone is present at relatively shallow depth, 3) a high temperature geothermal fluid is recharged at depth in the east of Ginyu fault and flows westward along the fault as indicated in Fig.1, 4) reinjected water in the western part of the field flows out the reservoir system to the west.

3. RESERVOIR MANAGEMENT

Steam quality of the produced fluid of wells ranges from 0.2 to 0.25 on average except wells whose feed zone depth locates in shallow zone (Horikoshi et al., 2005). All separated water is reinjected back into the formation at reinjection wells drilled in the western part of the field. Subsurface temperature gradually decreases westward and the elevation at reinjection wellheads are 730m to 760m a.s.l. that is lower than those of production well pads, 820 m to 850m, where produced fluids are separated (JGEA, 2000). Thus, the reinjection operation takes advantage of the topography for gravitational flow to reinjection wells. The main reinjection zone is located more than 600m west of the production zone, along the Ginyu fault.

Since the start of commercial operation of the plant in 1996, the total production rate of steam has decreased gradually with time. Thus, by 2005 three makeup wells were drilled for production and five for reinjection to maintain the specified output (Horikoshi et al., 2005). The decrease in steam production rate was estimated to be due to both reservoir pressure and temperature declines. The temperature drop may be caused by an excessive return of heat-depleted reinjection water to the production zone. Thus, tracer tests were conducted to examine and quantitatively evaluate the effects of reinjection water return to production zone (Horikoshi et al., 2005). The results showed that three reinjection wells, NT-D1, D2 and E4, significantly affected the production zone with quick return of reinjected water and return ratios of reinjected water to produced fluids as high as 34%. The other five reinjection wells, NT-D3, D4, D5, E6 and F1 have minor effects on the production wells and low mixing ratios, less than 4%. Then, a reinjection operation scheme was adopted such that the first three wells, NT-D1, D2 and E4, were mainly used to reinject waste water for two years from 1997 to 1999, with the aim of moderating reservoir pressure decline. However, the decrease of steam production was not mitigated with this change to the reinjection operation. Moreover a decrease in geochemical temperature and an increase in chloride concentration of the produced fluid were detected. This indicated excessive return of reinjected water of high chloride concentration and of low temperature to the production zone. At the same time, reservoir simulation studies revealed that there would be significant temperature decrease in the production zone. Furthermore, this simulation study suggested temperature decrease in the production zone could be avoided by reinjecting in the wells which have weak connectivity with production wells. Then, the reinjection operation since 2000 has been conducted using these five wells (NT-D3, D4, D5, E6 and F1).

Another feature of reservoir management at Ogiri is dry steam production from shallow wells whose feedzone depths are 100m to -100m a.s.l. Well C1 produced steam water mixture at flow rates of 35 t/h steam and 140 t/h water after completion of the well in 1983 (Horikoshi et al., 2005). However, production tests together with other wells in 1991 led the well to produce only steam at a flow rate of 85t/h. Two other wells drilled in the shallow zone, B5 and C3, also produce dry steam. However, their locations of feedzone are very close each other (within 50m), and showed interference among the wells. This suggested that the steam-dominated zone is relatively small in size with a limited capacity of steam production.

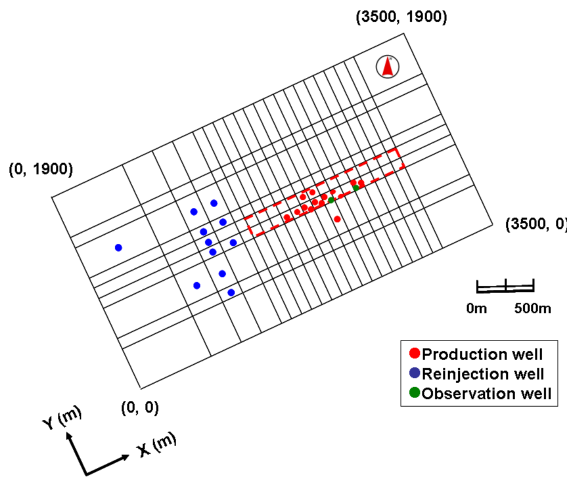

Figure 2: Plan view of grid system with feedpoint locations of wells.

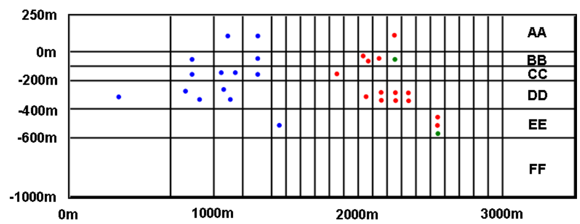

Figure 3: Cross section of grid system from AA to FF layers with feedpoint of wells.

4. NUMERICAL MODEL

4.1 Porous Medium Model

The numerical model of the Ogiri geothermal reservoir has a three-dimensional grid that covers an area of 5.5km by 3.9km with elevation 250m a.s.l. down to -2600m a.s.l. Figure 2 shows the plan view of the grid within the reservoir domain that excludes the peripheral blocks. The sizes of the grid blocks range from 100m×100m to 1000m×1000m with thicknesses of 100m to 1600m. The model was divided on a horizontal plane into 23 blocks for east-west and 11 blocks for south-north directions with seven layers. The layers were named from AA to GG which represent the top and the bottom layers of the grid, respectively. Areas representing the main flow paths of geothermal fluids by the Ginyu fault, the Ginyu auxiliary fault, the Sakkogawa fault and the NW1 fault were assigned the smallest blocks (Figs.1 and 2). On the other hand, a larger block was used in outer regions. The grid system was tilted by 27° from the east to north so that the main fault systems in ENE-SWS directions could be represented properly with rectangular coordinates.

Eleven (11) rock types were used in the model to assign different rock properties for the grid blocks on the basis of the hydrogeological characteristics of the Ogiri geothermal system.

Table 1: Permeability values for rock types.

Rock Type	Permeability (m^2)	
	kx, ky	kz
Ginyu fault (Production area)	3.70×10^{-13}	1.21×10^{-13}
Ginyu fault (Reinjection area)	3.36×10^{-14}	3.16×10^{-16}
Ginyu auxiliary fault	3.16×10^{-15}	2.03×10^{-15}
Sakkogawa fault	3.16×10^{-16}	3.16×10^{-19}
NW1 fault	3.81×10^{-14}	7.23×10^{-15}
Impermeable zone (Cap rock)	1.70×10^{-18}	3.56×10^{-19}
Makizono lava (Upper part)	2.98×10^{-15}	3.34×10^{-19}
Makizono lava (Lower part)	4.95×10^{-15}	8.06×10^{-15}
Iino lava	2.89×10^{-16}	1.17×10^{-15}
Basement rock (Shimanto Group)	2.56×10^{-18}	1.00×10^{-14}
Top layer	1.70×10^{-18}	3.56×10^{-19}

Table 2 : Parameters for grid blocks processed with MINC method.

Matrix	
Permeability	$k_m = 10^{-15}$ m^2
Porosity	$\varphi_m = 10$ %
Fracture	
Permeability	$k_{fx,\,fy} = 3.70\times10^{-13}$ m^2, $k_{fz} = 1.21\times10^{-13}$ m^2
Porosity	$\varphi_f = 50$ %
Spacing	λ= 50m
Nested volume element	
Volume ratio	Fracture : Matrix1 : Matrix2 = 0.02 : 0.2 : 0.78
Relative Permeability	
Corey curves	$S_{lr} = 0.30$, $S_{sr} = 0.10$

Table 1 summarizes the permeability values of each rock type assigned to the numerical model. Kumamoto et al. (2008a) investigated the rock properties in the Ogiri geothermal area in detail. The optimum values of rock permeability in the field were estimated through inverse analysis for natural state by using the code iTOUGH2 (Finsterle, 1999), therefore those values except for the Ginyu auxiliary fault with permeability k_x=k_y= 3.16x10^{-15} m^2, and k_z= 2.03x$10^{-15}$$m^2$ were used here in constructing the numerical model. Thermal conductivity was given in a range from 1.6 to 3.0W/m°C. Porosity of 10%, density of 2500kg/m^3 and specific heat of 1050 J/kg°C were given to all rock types.

4.2 MINC Model

We applied the MINC method (Pruess et al.,1999) to the grid blocks indicated by the red dotted line that represents the main production zone of Ginyu Fault as shown in Fig.2. The MINC model has the same grid system as the porous medium model. Kumamoto et al. (2009) examined the effectiveness of the method in the Ogiri numerical model by applying the MINC process for all grid blocks corresponding to Ginyu Fault except the layer AA. The results indicated that the steam-water two-phase zone was formed only in the shallow layers and water single phase remains in other deeper layers throughout the history matching simulation period. Thus, the MINC method being effective for simulating two-phase conditions was applied only to BB and CC layers in the model. For the grid blocks being processed with the MINC method, matrix permeability of $10^{-15}$$m^2$ and intervals of fracture domain of 50m were given (Kumamoto et al., 2009). Fracture permeability values of grid blocks processed with the MINC method were given the same values as those of the porous medium model in which the rock type of the Ginyu fault (Production area) was assigned: 3.70x10^{-13} m^2 for k_x and k_y, and 1.21x10^{-13} m^2 for k_z (Table 1). Parameters of the grid block processed with the MINC method are summarized in Table 2. Grid blocks of porous type in the model were given with parameters of the porous medium model

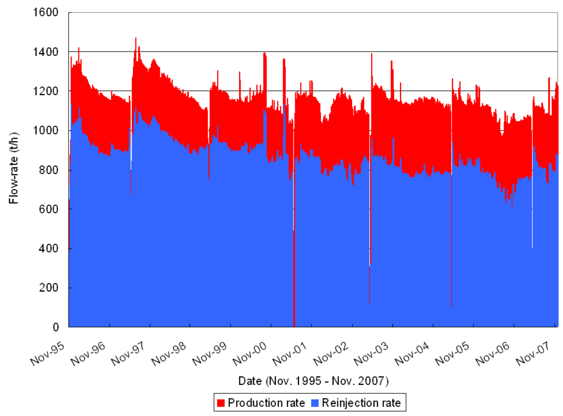

Figure 4: Flow rate history of production and reinjection in Ogiri.

4.3 Location and Depth of Feedzone

Figure 2 also presents the locations of feedzones for production, reinjection and observation wells in the reservoir domain of the numerical model. Production wells were drilled by targeting the Ginyu fault, and their feedzones are located within a relatively small region of horizontal plane of 800 m by 200 m. Two monitoring wells are located in the east of the production zone. The vertical slice of the model in Fig.3 shows the model from BB to FF layers and the feed zone depths of the wells. Below FF layer, there is the bottom layer GG with a depth from -1000m to -2600m a.s.l. Most production and reinjection wells have their feed zone in BB, CC and DD layers. Observation well KE1-13 in BB layer monitors the pressure and temperature of the shallow reservoir that is characterized by the presence of a two-phase zone at the top. Observation well KE1-19 indicates deep reservoir characteristics of single-phase water conditions.

The codes Mulgeom and Mulgraph (O'Sullivan and Bullivant, 1995) were used as pre- and post- data processors.

5. SIMULATION CONDITIONS

We carried out history-matching simulations with the two models; the porous medium model and the MINC model. The calibration period is 22 years from July 1984 to August 2006. For the initial condition of the numerical model, the natural state model for the Ogiri geothermal reservoir obtained through the preexploitation modeling with porous medium model was employed for both models (Kumamoto et al., 2008b).

For the boundary conditions of the model, constant pressure of 9.807×10^4 Pa and temperature of 75°C at the top surface were given The lateral boundaries were assumed to be impermeable with respect to mass and adiabatic to heat. Constant pressure conditions were given to the grid blocks located along the lateral boundary on the west of reinjection zone along NWN-ESE direction. Outflow of reinjected water from the model to westward can be realized with this condition. A conductive heat flux of 0.432W/m^2 was assigned to the grid blocks of the bottom layer on the southern part of Sakkogawa Fault. The remaining bottom layer blocks were assigned a heat flux of 0.0432W/m^2.

Mass recharge was specified at two blocks of the bottom layer: 30kg/s of 1047.1kJ/kg (242^{o}C) for a grid block located in the eastern part and 55 kg/s of 1062.7 kJ/kg (245^{o}C) for the other block located in the deep zone of the production area. Therefore, a total mass of 85kg/s of about 240^{o}C water was recharged at depth into the model. The flowrate histories of respective production and reinjection wells were used as sinks/sources. Figure 4 shows the histories of production and reinjection flow rates. Low temperature reinjection water of 546.3kJ/kg (saturated water of 130^{o}C) was reinjected on the basis of the actual operating condition.

6. RESUTS AND DISCUSSION

Simulated results were compared against the measured pressure and temperature histories in two observation wells, KE1-19 and KE1-13. Both wells are located in the central part of the Ginyu reservoir (Figs. 2 and 3), but their feed zone depths are different – in the deep hot-water reservoir for Well KE1-19, and in the two-phase shallow zone for Well KE1-13. Pressure and temperature histories of Well KE1-19 after 1995 are compared with the simulated results in Fig.5. Measured pressure shows gradual decrease with time since 1996 with a quick drop in 1999. The sudden drop of pressure in 1999 corresponds to the changes in reinjection well operation. On the other hand, simulated pressures for both model show a quick drop at early times, then their rates of decrease are moderated. The pressure starts decreasing gradually with time after 2000. Simulated pressure in the porous medium model shows higher value in the middle times, and shows the lowest values in the later period. Simulated pressure in the MINC model shows a relatively good match over the whole production period.

Comparison of temperatures in Well KE1-19 is shown in Fig.6. Measured temperatures show a variation over a range from 225 to 230^{o}C. Saturation pressure of water with respect to this temperature range is 25.5 to 28.0 bar which is lower than the measured pressure as shown in Fig.5. Thus, fluid in reservoir of this depth remains single-phase water. The simulated temperatures do not show differences between the models and also remain constant throughout the simulation period although at a level several degrees C higher than the measured one.

Feedzone pressures in Well KE1-13 are compared between measurement and simulation in Fig. 7. Pressure measurement was continued from 1997 until March 2002. During this period, observed pressure values gradually decreased with time and show a quick drop in 1999 the same as in KE1-19. Simulated pressures with the MINC model show a good fit with the measurements. However, those with the porous medium model show higher values throughout the simulation period, and match with the measurement is rather poor. Figure 8 compares the simulated and measured temperatures for Well KE1-13. Simulated temperatures from the MINC model also give better match to the measurements compared with those from the porous medium model. The quick drop in measured temperature in 1999 is reproduced relatively well by the MINC model. This temperature drop corresponds to that of pressure as shown in Fig.7. The simulated temperature continues decreasing down to about 200^{o}C in 2006. This temperature decrease can be attributed to cooling due to extraction of heat from reservoir for vaporization to form steam in the two-phase zone. The simulation with the porous medium model could not be continued beyond June 2006 as the fluids in grid blocks depleted in the shallow zone and pressure in the grid blocks dropped significantly. However, the MINC model could continue the simulation.

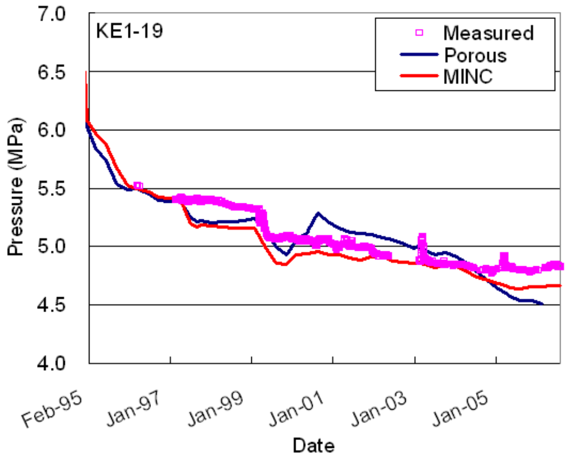

Figure 5: Comparison of simulated pressures and measured one in Well KE1-19.

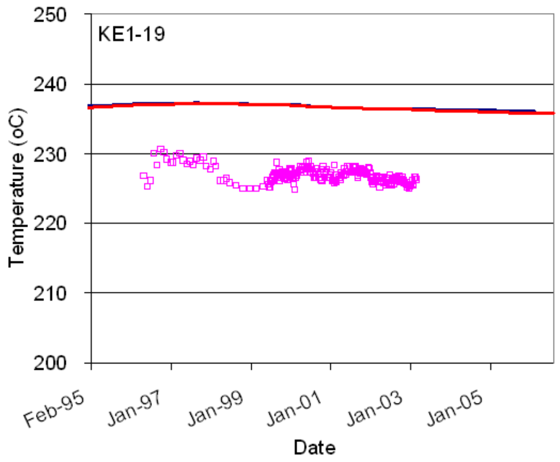

Figure 6: Comparison of simulated temperatures and measured one in Well KE1-19.

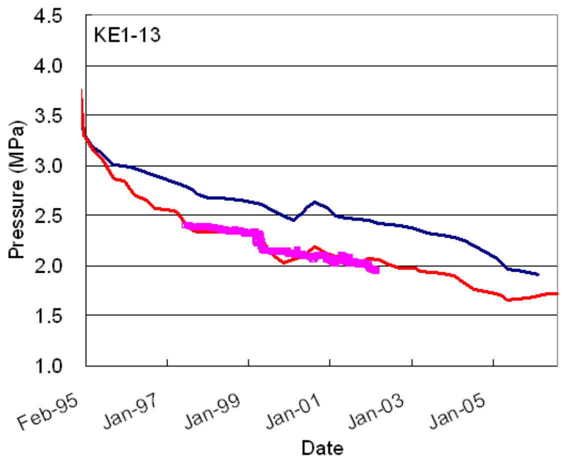

Figure 7: Comparison of simulated pressures and measured one in Well KE1-13.

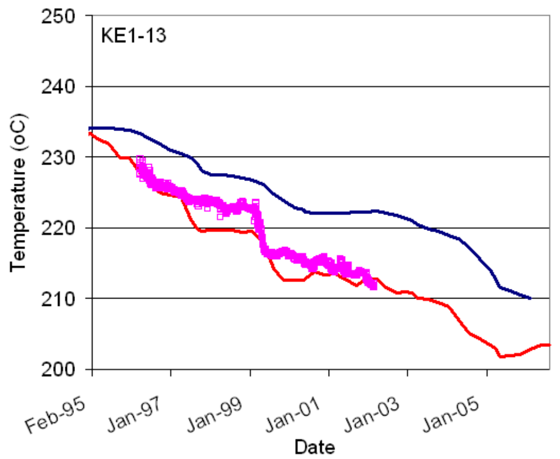

Figure 8: Comparison of simulated temperatures and measured one in Well KE1-13.

Figure 9 shows a plan view of the simulated temperature distributions of BB layer in 1996 and in 2006. The high temperature zone in 1996 extends along the Ginyu fault zone and temperature decreases towards the west. In 2006, temperature generally decreases compared with that in 1996 and the low temperature zone below 200°C extends eastward along grid blocks corresponding to the Ginyu fault in the main reservoir. Figure 10 presents vapor saturation distributions in BB layer in 2006. Vapor saturation shows a high value of 0.9 in the middle of the Ginyu fault which supports the production of high enthalpy fluids of wells from the shallow zone. The figure indicates water invasion into the two-phase zone from west to east. This may be caused by return of reinjected water into the production zone.

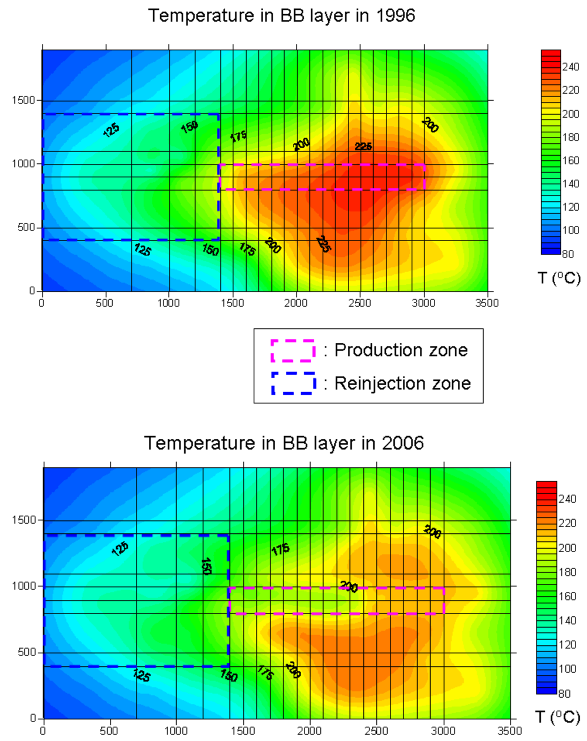

Figure 9: Simulated temperature distributions in BB layer in 1996 and 2006.

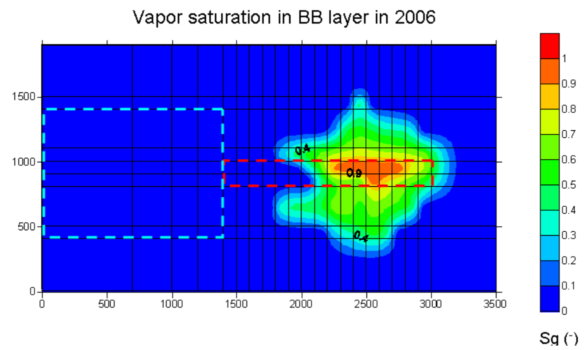

Figure 10: Simulated vapor saturation distribution in BB layer in 2006.

7. CONCLUSIONS

History matching simulation for the Ogiri geothermal reservoir was conducted using three-dimensional numerical models of porous medium and fractured types. The MINC method was partially built in the shallow zone of the reservoir where the steam-water two-phase zone is formed. Simulated results with the MINC model show reasonable match to the measured pressure and temperature of observation well KE1-13 located in the shallow reservoir.

REFERENCES

Finsterle, S.: "iTOUGH2 User's Guide, *Report LBNL-40040* Lawrence Berkeley National Laboratory, University of California, Berkeley, CA(2000).

Goko, K.: Geological analysis and evaluation of the Ogiri geothermal structure in the Kirishima geothermal area, *Resource Geology*, *(in Japanese with English abstract)*, **45**, (1995), 41-52.

Goko, K.:Structure and hydrology of the Ogiri field, West Kirishima geothermal area, Kyushu, Japan, *Geothermics*, 29, (2000), 127-149.

Hazama, Y., Nagao, S., Abe, I., Monden Y. and Nobumoto, R.(1988):Reservoir Simulation on the Kirishima geothermal field, *Proceedings International Symposium on Geothermal Energy, Kumamoto and Beppu*, (1988), 140-143

Horikoshi, T., Takayama, J., Takeshita, K., Goko, K., and Yoshizawa, H.:An analysis of the geothermal structure of the Ogiri geothermal field based on the surveys and operational data of the Ogiri Power Station after its commencement, *Resource Geology (in Japanese with English abstract)*, **55**, (2005), 25-38.

Japan Geothermal Energy Association(JGEA): Directory of Geothermal Power Plant in Japan (New Edition), *Japan Geothermal Energy Association (in Japanese)*, (2000), 254pp.

Kumamoto, Y., Itoi, R., Tanaka, T., and Hazama, Y.: Development of the Optimum Numerical Reservoir Model of the Ogiri Geothermal Field, Kyushu, Japan, Using ITOUGH2, *Proceedings, 33th Workshop on Geothermal Reservoir Engineering*, Stanford University, Stanford, CA(2008a)

Kumamoto, Y., Itoi. R, Horne, R. and Hazama, Y.: Numerical Modeling of the Ogiri geothermal system, Kyushu, Japan , *Trans. Geothermal Resources Council*, **32**, (2008b), 449-458

Kumamoto, Y., Itoi,R., Tanaka, T. and Hazama, Y.:Modeling and Numerical Analysis of the Two-phase Geothermal Reservoir at Ogiri, Kyushu, Japan, *Proceedings, 34th Workshop on Geothermal Reservoir Engineering*, Stanford University, Stanford, CA(2009)

O'Sullivan, M. J. and Bullivant, D. P.: A graphical interface to the TOUGH2 family of flow simulators, *Proceedings*, TOUGH Workshop 1995, Lawrence Berkeley Laboratory Report LBL-37200, CA(1995)

Pruess, K., Oldenburg, C. and Moridis, G. : TOUGH2 User's Guide, Version 2.0, *Report LBNL-43134*, Earth Sciences Division, Lawrence Berkeley National Laboratory, University of California, Berkeley, CA(1999)

Yano, Y. and Ishido, T.: Numerical Modeling of the Evolution of Two-Phase Zones Under a Fractured Caprock, *Geothermics*, **24**, (1995), 507-521